

Stabilization of a low-frequency instability in a dipole plasma

D.T. GARNIER¹, A.C. BOXER², J.L. ELLSWORTH²,
A.K. HANSEN¹, I. KARIM², J. KESNER², M.E. MAUEL¹,
E.E. ORTIZ¹ and A. ROACH²

¹Department of Applied Physics and Applied Mathematics, Columbia University,
New York, NY 10027, USA

²Plasma Science and Fusion Center, MIT, Cambridge, MA 02139, USA
(kesner@psfc.mit.edu)

(Received 11 September 2007 and accepted in revised form 9 November 2007)

Abstract. Low-frequency fluctuations are observed in a plasma confined by a strong dipole magnet and containing an energetic high-pressure population of trapped electrons. The quasi-coherent fluctuations have frequencies characteristic of drift frequencies of the lower temperature background plasma and have large toroidal and radial extent. They are excited throughout a wide range of plasma conditions determined by the level of neutral gas pressure. However, for a sufficiently high rate of neutral gas fueling, the plasma density profile flattens and the fluctuations disappear.

1. Introduction

Low-frequency fluctuations are often present in magnetic confinement systems and can result in substantial particle and energy transport. In systems that lack magnetic shear and in which plasma compressibility is not significant, the so-called ‘universal’ instability is always present [1]. In systems with substantial compressibility, however, such as a levitated dipole, all low-frequency modes can be stable.

High-beta confined plasma has been created and maintained in a dipole field device [2] using multi-frequency electron cyclotron resonance heating (ECRH). These plasmas contain a low-density hot electron population which accounts for most of the plasma stored energy and a cool background plasma that accounts for most of the density. The free energy of the hot component can drive ‘hot electron interchange’ (HEI) modes as has been reported in [2]. In this article we will discuss low-frequency quasi-coherent modes that are sometimes seen in the Levitated Dipole Experiment (LDX) and which are believed to be driven by the free energy of the background plasma.

The LDX [3] has a closed field line magnetic topology in which a large expansion of magnetic flux gives rise to a substantial plasma compressibility, i.e. a large variation in the flux tube volume ($V(\psi) = \oint dl/B$ with ψ the magnetic flux), which provides MHD stability. Figure 1 shows the LDX magnetic field line geometry and the RF resonances. The confining magnetic field is provided by the floating coil, a superconducting coil that is internal to the plasma. The mean radius of

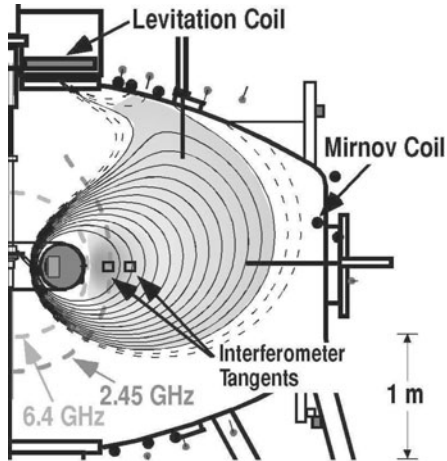


Figure 1. Schematic of the LDX experiment showing magnetic field lines, diagnostics and RF resonant surfaces at 2.45 and 6.4 GHz. An X-point ring null, or magnetic separatrix, is formed when the levitation coil is charged.

the coil current is $R_c = 0.34$ m and in the experiments described below the coil was supported by three thin supports which intersect the plasma in the high field region. The cryostat surrounding the coil extends along the midplane from 0.22 m to 0.58 m with limiters at the inner and outer locations. A second coil, known as the levitation coil, sits above the vacuum chamber. When the levitation coil is sufficiently energized it introduces a magnetic separatrix into the vacuum chamber which contains a ring null and serves to limit the plasma. A low-frequency instability discussed below has been observed with or without the ring null although the window of parameters in which these modes are observed shifts.

For plasma heated by ECRH the density is limited by the requirements of wave accessibility such that the electron plasma frequency does not exceed the local electron cyclotron frequency along the trajectories of the propagating waves. The experiments reported here were heated by 5 kW evenly divided between 2.45 GHz and 6.4 GHz with cutoff densities of $7.4 \times 10^{16} \text{ m}^{-3}$ and $5.1 \times 10^{17} \text{ m}^{-3}$, respectively. The 6.4 GHz source is resonant at the midplane close to the coil at $R = 0.63$ m (Fig. 1) whereas the 2.45 GHz source is resonant at $R = 0.83$ m. The coupling to the plasma is weak and the waves will bounce many times before depositing their energy, leading to toroidally symmetric heating. Additionally, mode conversion to Bernstein waves might permit heating when the density exceeds a critical value [4] as seen in other dipole experiments [5].

For sufficiently low density, the resulting plasma will contain a hot electron species, typically $T_{\text{eh}} > 10$ keV, immersed in a cool background plasma. Plasma losses are predominantly to the supports which are observed to glow during RF heating. The hot electron component forms a high beta plasma ($\beta_{\text{max}} \sim 20\%$), which is determined from magnetics, and the location of the hot electrons are verified by x-ray imaging [2]. Hot electron energies are inferred from the frequency of resonantly driven hot-electron-interchange modes and are consistent with measured x-ray spectra. The hot electrons form a ring that is localized to the outer midplane while the background plasma is isotropic and tends to fill the entire the flux volume.

The hot species is anisotropic and subject to hot-electron-interchange modes [2] that resonate with the hot electron drift frequency [6, 7]. The background plasma may be unstable and stability is determined by the background plasma profiles: MHD modes are driven by the pressure gradient [8]; centrifugal instability appears in a rotating plasma and depends on the density gradient [9–11]; and drift frequency modes such as the entropy mode appear in an MHD stable plasma and depend on the ratio of temperature and density gradients, defined by the parameter $\eta \equiv d \ln T_e / d \ln n_e$ [12–14]. The entropy mode is expected to be present in all regimes of collisionality [13] and these modes are predicted to be interchange-like at low beta. For the background plasma these instabilities are weak and are expected to saturate nonlinearly to form a turbulent state. In this article, we will focus on the observation of low-frequency collective modes in the LDX ECR-heated plasmas.

2. Experimental results

In the parameter range of LDX the electrons are collisional while the deuterium ions can be collisionless. From microwave interferometry and edge swept Langmuir probe measurements $T_e \sim 10$ eV and $n_e \sim 2 \times 10^{16} \text{ m}^{-3}$, and we can determine $\nu_e \sim 20$ kHz, $\nu_i \sim 0.3$ kHz. Neutrals penetrate deeply into the plasma and the density profile is observed to be affected by the edge neutral pressure. Neutrals can pitch-angle scatter hot electrons but ion–neutral collisions are unimportant ($\nu_{in} < 100$ Hz).

Figure 2 illustrates a discharge in a well-conditioned machine ($p_0 < 10^{-6}$ Torr before the discharge) with the levitation coil powered so as to produce a diverted magnetic geometry. In a typical discharge, about 5 kW of ECRH power (Fig. 2(a)) was applied to the plasma at 2.45 GHz and 6.4 GHz which is resonant on the outer midplane 25 cm and 5 cm, respectively, from the floating coil. A deuterium prepuff raises the neutral pressure so that $p_0 > 10^{-6}$ Torr appears to be necessary to create a plasma that will transition into the high beta regime characterized by the stabilization of the hot electron interchange mode [2]. Thereafter, the plasma pumps the neutral background, which drops back to $p_0 < 10^{-6}$ Torr. This discharge is characterized by an early transition to the high beta regime [2], indicated by a build-up of plasma diamagnetism (Fig. 2(b)). Following the termination of heating at $t = 8$ s the plasma density falls precipitously (see, for example, Fig. 4(d)) while the plasma diamagnetism falls slowly (Fig. 4(b)) indicating that whereas most of the density resides in background ‘cold’ plasma (which is flowing rapidly to the supports) most of the plasma energy content resides in the hot electron species.

Figure 2(e) shows the Mirnov coil signal obtained from a coil located just inside of the vacuum chamber wall at the midplane. The time–frequency-domain (TFD) plot for this signal (derived from Fourier analysis with a sliding time window) is shown in Fig. 2(f). A similar spectrum is seen on a broadband visible photodiode detector located on the outer plasma midplane. For $t < 6$ s we observe a mode whose frequency rises to $f \sim 4$ kHz. Gas fueling was disabled at $t = 6$ s, at which time the base pressure is 3×10^{-7} Torr and thereafter the background pressure drops by about 10%. The mode frequency was observed to rise abruptly after $t = 6$ s.

A steepening of the density profile is often seen to accompany a decrease in fueling rate. Figure 2(d) exhibits density measurements obtained from a multi-chord interferometer with chords that are tangent to flux tubes at major radii of $R_i = 0.77$ m and 0.96 m, respectively. After the gas fueling turns off ($t = 6$ s) the

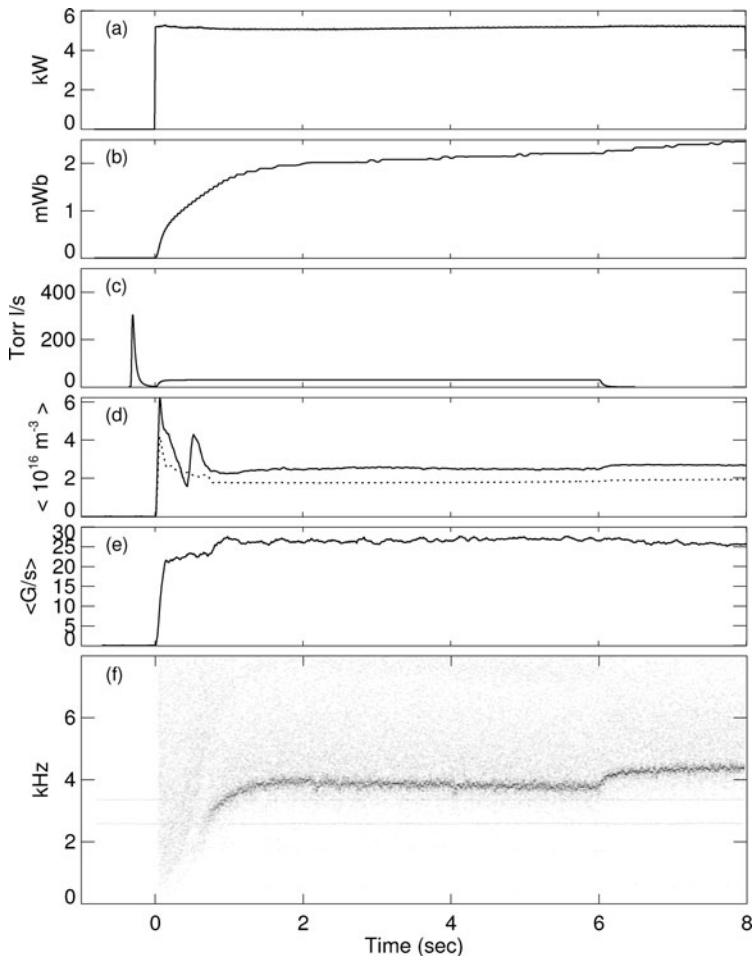


Figure 2. Traces for discharges 60714020 showing (a) ECRF heating power, (b) plasma diamagnetism, (c) neutral gas fueling rate, (d) two line-averaged densities from chords at $R = 0.77$ and 0.96 m (dotted), (e) ‘Mirnov’ magnetic fluctuation signal and (f) time–frequency-domain plot for this discharge.

inner-most chord is seen to rise by approximately 10%. The implied steepening of the density profile indicates that the reduction of neutral pressure is accompanied by a change in the source profile.

An array of Mirnov coils placed at 45° intervals on the midplane and at a radius of 2.5 m has been analyzed using ‘fixed probe pair’ analysis [15] (Fig. 3). This analysis indicates an $m = 1$ mode. However, as the Mirnov coils are located far from the plasma they may not be sensitive to higher mode number modes that may be present.

The mode is seen to propagate in the electron diamagnetic direction. A tangentially viewing radial array of photodiodes also picks up the mode on all channels. All channels appear to be in phase indicating a broad radial eigenmode.

In a second experiment, a 1 s gas puff was introduced during a similar discharge. The initial neutral pressure in this discharge is relatively high (7×10^{-7} Torr) and the turbulent state seen early in the discharge ($t < 3$ s) exhibits two modes that are less

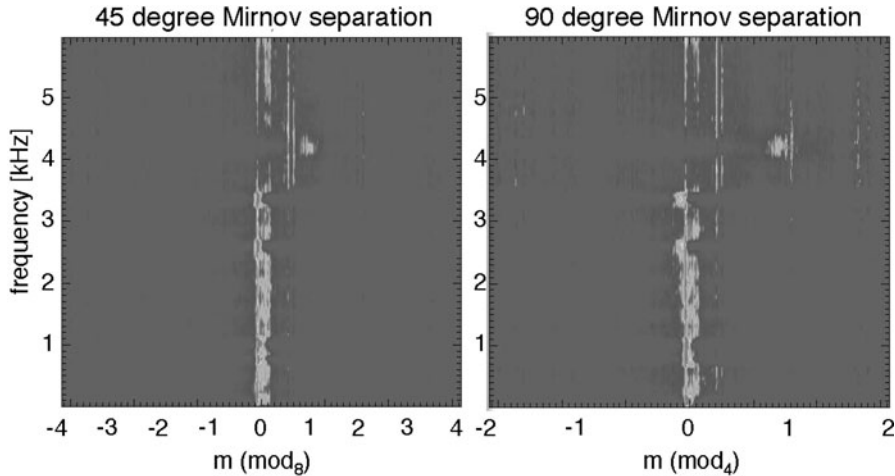


Figure 3. Correlation of Mirnov probes separated by 45° and 90° for discharge 60714020.

coherent than seen in discharges with lower base pressure. At $t = 3$ s a strong 1 s gas puff is applied (Fig. 4(c)). Thereafter, the density rises and the turbulence turns off. The Mirnov signal (Fig. 4(e)) indicates a sharp drop in the fluctuation level with an exponential decay of ~ 50 ms and the associated TFD plot (Fig. 4(f)) indicates that this reduction of turbulence extends across the entire range of frequencies below 10 kHz leaving only a low level of incoherent turbulence. The diamagnetic signal also falls, but with a slower ~ 600 ms decay. Enhanced hot electron loss probably results from increased pitch-angle scatter on neutrals and subsequent scrape-off on the supports. A gradual return in the level of turbulence is observed after the puff ends at $t = 4$ s.

A multi-chord interferometer (Fig. 4(d)) indicates that after the gas fueling rises at $t = 3$ s the outer-most chord (at $R_i = 0.96$ m) rises up to close to the level of the inner-most chord ($R_i = 0.77$ m), indicating a flattening of the density gradient. This is consistent with the previous observation from Fig. 2 where it was observed that a decrease of gas fueling (at $t = 6$ s) leads to an increase in the density gradient. The appearance of quasi-coherent low-frequency turbulence thus appears to be related to the density profile.

The modes are only seen in a range of gas feed and vacuum conditions, i.e. for the edge neutral pressure, p_0 , in the range 3×10^{-7} Torr $< p_0 < 8 \times 10^{-7}$ Torr in the presence of a ring null. In the absence of the ring null (when the levitation coil is not excited) the unstable range of neutral pressures widens. Additionally, these modes are only present when heating at 2.45 GHz is utilized. Examination of the multi-chord interferometer data indicates that the 2.45 GHz heating source tends to reduce the steepness of the density profile.

3. Discussion

Instability can result from several sources including pressure-gradient-driven MHD modes, rotation-driven MHD modes that depend on the density gradients or profile-driven drift modes that depend on η . These are discussed briefly below. Observations suggest stability depends on having appropriate density and temperature profiles.

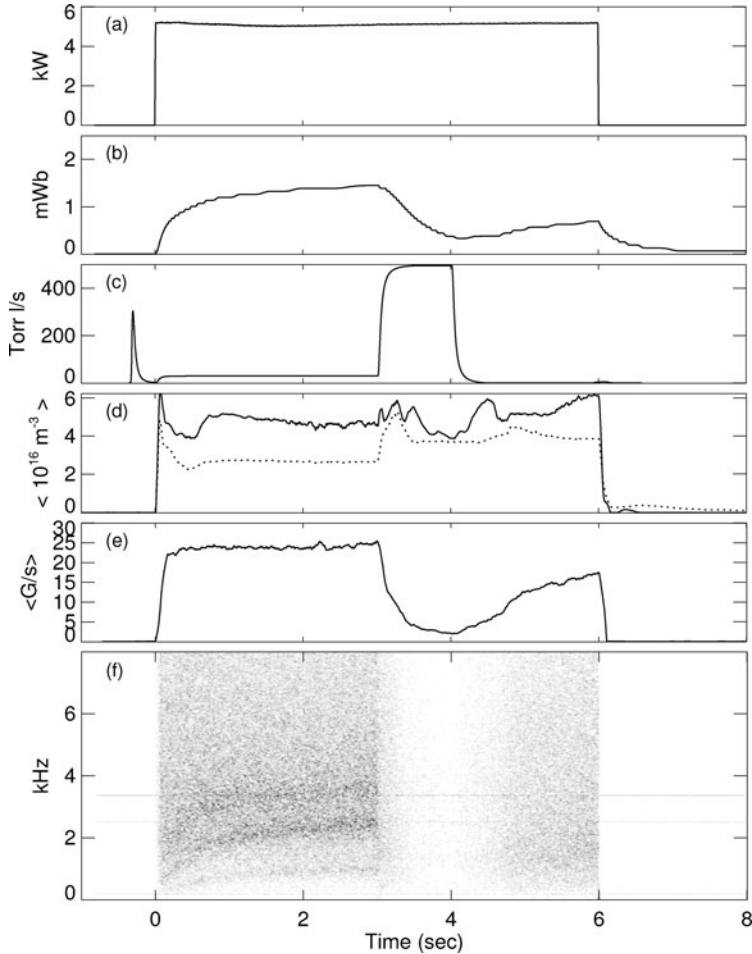


Figure 4. Traces for discharge 60714009 showing (a) ECRF heating power, (b) plasma diamagnetism, (c) neutral gas fueling rate, (d) two line-averaged densities from chords at $R=0.77$ and 0.96 m (dotted), (e) ‘Mirnov’ magnetic fluctuation signal and (f) time–frequency-domain plot for this discharge.

Similar results are observed when the ring null is not present but the ring null appears to facilitate the turn-off of low-frequency turbulence. Additionally, we observe that a dipole-confined plasma can be free of low-frequency fluctuations.

Unstable MHD modes can be excited in the ‘bad’ curvature region that exists between the pressure peak and the outer wall or separatrix. The MHD stability criterion for the background non-rotating plasma may be written as $-d \ln p_b / d \ln V \leq 5/3$ and the presence of a hot electron species only leads to a small modification of this criterion [8, 16]. In the nonlinear state, large-scale convective cells with toroidal mode number $n = 1$ can form [17]. A toroidal mode number of $m = 1$ would appear in the laboratory frame at 4 kHz for a rotation of Mach number $M = v_{\text{rot}}/v_{\text{thermal}} \sim 1.1$ with v_{th} the ion thermal speed for $T_i \sim 10$ eV. Furthermore, in the presence of MHD-driven flux tube mixing, the density will obtain a

profile which is characterized by an equal number of particles per flux tube [17], i.e. $-d\ln n_b/d\ln V = 1$.

The linear properties of drift frequency modes in a closed-field-line system such as a dipole have been examined [12–14, 18, 19]. A low-frequency mode known as the ‘entropy mode’ is predicted to appear beyond the pressure peak when $\eta \equiv d\ln T_e/d\ln n_e < 2/3$ and with a frequency (ω) and growth rate (γ) $\omega \sim \gamma \sim \omega_{\text{di}}$ with $\omega_{\text{di}} = (k_{\perp}\rho_i)v_{\text{th}}(\kappa + \nabla_{\perp} \ln B)$ the magnetic drift frequency, and ρ_i the ion gyroradius. The linear growth rate for entropy modes is found to be a maximum for $k_{\perp}\rho_i \sim 1$ [18]. Nonlinear simulations of the entropy mode [20] indicate that, when unstable (i.e. $\eta < 2/3$), it can create structures of $\sim 20\rho_i$ which, for an estimate of $T_i \sim 10$ eV, is equivalent to a toroidal mode number of $m \sim 60$. Such high mode numbers would not be observable on the Mirnov loops. The turbulence features would rotate with the plasma leading to a real frequency of 4 kHz for $M \sim 0.02$.

Centrifugal modes have low frequencies in the rotating plasma frame of reference, and the appearance of these modes depends on the rate of plasma rotation and the steepness of the density gradient [11]. Alfvén waves, if present, would have substantially higher frequencies than observed, $f_A \sim V_A/m \sim 10^8\text{--}10^9$ Hz with V_A the Alfvén speed and m the toroidal mode number.

4. Conclusion

In conclusion, the levitated dipole presents a new and promising approach to magnetic confinement. It is well known that energy confinement can be degraded by low-frequency plasma turbulence driven by the free energy of density and temperature gradients. In this article we present the first observations of low-frequency quasi-coherent modes in a dipole and the conditions under which these modes are seen. We do not have sufficient profile measurements to make a specific identification of the observed mode and this task will be the focus of future research.

In future LDX experiments the loss of background plasma to the supports of the internal ‘floating’ coil will be eliminated by magnetic levitation of the floating coil. Eliminating plasma losses along the field lines is expected to lead to hotter and more dense plasmas with lower fueling and possibly with increased density gradients.

Acknowledgements

This work was supported by US DOE grants DE-FG02-98ER54458 and DE-FG02-98ER54459.

References

- [1] Antonsen, T. M. 1978 *Phys Rev Lett.* **41**, 33.
- [2] Garnier, D. T., Hansen, A., Mauel, M. E., Ortiz, E. E., Boxer, A. C., Ellsworth, J., Karim, L., Kesner, J., Mahar, S. and Roach A. 2006 *Phys. Plasmas* **13**, 056111.
- [3] Garnier, D. T. et al. 2006 *Fusion Eng. Design* **81**, 2371.
- [4] Ram, A. and Schultz, S. 2000 *Phys. Plasmas* **7**, 4084.
- [5] Ogawa, Y. et al. 2003 *J. Plasma Fusion Res.* **79**, 643.
- [6] Krall, N. A. 1966 *Phys. Fluids* **9**, 820.
- [7] Berk, H. L. 1976 *Phys. Fluids* **19**, 1255.

- [8] Garnier, D. T., Kesner, J. and Mauel, M. E. 1999 *Phys. Plasmas* **6**, 3431.
- [9] Siscoe, G. K. and Summers, D. 1981 *J. Geophys. Res.* **86**, 8471.
- [10] Hill, T. W., Dessler, A. J. and Maher, L. H. 1981 *J. Geophys. Res.* **86**, 9020.
- [11] Levitt, B., Maslovsky, D. and Mauel, M. E. 2005 *Phys. Rev. Lett.* **94**, 175002.
- [12] Kesner, J. 2000 *Phys. Plasmas* **7**, 3837.
- [13] Kesner, J. and Hastie, R. J. 2002 *Phys. Plasmas* **9**, 395.
- [14] Simakov, A., Catto, P. J. and Hastie, R. J. 2001 *Phys. Plasmas* **8**, 4414.
- [15] Beall, J. M., Kim, Y. C. and Powers, E. J. 1982 *J. Appl. Phys.* **53**, 3933.
- [16] Krasheninnikova, N. and Catto, P. J. 2005 *Phys. Plasmas* **12**, 32101.
- [17] Pastukhov, V. P. and Chudin, N. V. 2001 *Plasma Phys. Rep.* **27**, 907.
- [18] Ricci, P., Rogers, B., Dorland, W. and Barnes, M. 2006 *Phys. Plasmas* **13**, 62102.
- [19] Simakov, A., Hastie, R. J. and Catto, P. J. 2002 *Phys. Plasmas* **9**, 201.
- [20] Ricci, P., Rogers, B. and Dorland, W. 2006 **97**, 245001.